PMSST

Journal of Applied Science, Innovation & Technology (JASIT)

Journal homepage: https://prakritimitrango.com/documents-reports-and-publications/journal/

Research article

Comparative study on removal of cationic and anionic dyes using biochar synthesized from dry leaves of *Legerstroemia speciosa*: Kinetics, isotherm and thermodynamic study

Pooja Adwani[1*], Bhanusree B[1], Meenakshi[1], Shakti Singh[2*], Jiwan Singh[1]

[1]*Department of Environmental Science, Babasaheb Bhimrao Ambedkar University, Lucknow-226025, India*

[2]*Department of Chemical Engineering, University of Seoul, Seoul 02504, Republic of Korea*

OPEN ACCESS

ARTICLE INFOR

Article history:
Received: 27 November 2024
Revised: 9 December 2024
Accepted: 10 December 2024
Published online: 28 December 2024

Keywords:
Methylene blue (MB);
Methylene orange (MO);
Biochar;
Adsorption;
Kinetics;
Isotherm

ABSTRACT

The produced material was used in this study as an adsorbent to remove the organic pollutants such as methylene blue (MB) and methyl orange (MO) from an aqueous solution. Scanning electron microscopy (SEM), Fourier transform infrared spectra (FTIR), X-ray diffraction (XRD), Particle size analysis (PSA) characterization techniques were used to analyze morphological, chemical structure, nature and size of particles of an adsorbent. The dose study was performed to check optimum dose for removal of cationic dye (CD) and anionic dye (AD) which was 1g/L and 3 g/L, respectively. Different isotherm studies (Langmuir, Freundlich, Temkin, Dubinin-Radushkevich) were performed and confirm that the adsorption process followed Langmuir isotherm which means that adsorption is monolayer it was again confirmed by value of R^2 (0.98 for MB and 0.95 for MO). Kinetics study revealed that Pseudo-second-order (PSO) followed for both MB and MO which confirmed chemisorption. High value of ΔH^o was observed for MB confirmed that adsorption process is chemisorption. Negative value of ΔS^o revealed that process is spontaneous in nature. High removal percentages of MB and MO were achieved 95.7% and 94%, respectively, revealed that Legerstroemia speciosa biochar (LSB) is very effective adsorbent for the removal of organic pollutants (MB and MO).

1. Introduction

Dyes are natural or synthetic organic molecules with high molecular weights and intricate molecular structures. In general terms, the two primary ways that dyes are categorized are either by their chemical composition or by how they are applied to various substrates, including textile fibres, paper, leather, plastics etc. Azo, Anthraquinone, Indigo, Phthalocyanine, Sulphur, Jia chuan, Triaryl methane, Heterocyclic are major categories of the dyes.. Based on the application of dyes, they can be reactive, acid, soluble, insoluble, oxidation, disperse, polycondensation and fluorescent dyes (Long et al., 2020). Azo dyes have widespread applications in the textile, paint, leather, pulp paper, cosmetics, medicinal and dyeing sectors along with other common industrial products like rubber, petroleum etc. (Su et al., 2014). As compared to the natural dyes, azo dyes are more stable against light, temperature changes, chemicals, detergents, and microbial deterioration. They are also less expensive and easier to use. Azo dyes are most extensive and versatile group of synthetic dyes. They are composed of one or more sulfonic (SO^{3-}) and azo (-N=N-) bonds that are joined to various functional groups like amino, methyl, nitro, hydroxyl, sulfoxyl and carboxyl (Alhujaily et al., 2020). As one common azo dye in the printing and dyeing industry and potential in causing serious effects in ecosystem and living beings, MO and MB is an organic, heterocyclic, synthetic and high water-soluble anionic and cationic dyes, respectively. Typically, MB is a toxic dye (Russo et al., 2016), large amount of which (more than 7.0 mg/kg) can cause nausea, high pressure of blood, abdominal pain and mental health issue (Bharagava et al., 2021; Quansah et al., 2020, Oz et al., 2011). The reactive singlet oxygen that is produced by photo-sensibilized of MB by white light it may damage the DNA structures resulting threatening the human health (Albadarin et al., 2017). MO is an obstinate dye that can induce dermatitis, allergy, intestinal cancer and hypersensitivity in living things (Shabaan et al., 2020). By catalysing the reductive dissociation of the azo bond, reductive enzymes in the liver can produce aromatic amines, which may be the first step toward the development of intestinal cancer. MO is therefore categorized as an allergenic chemical that could trigger skin dermatitis upon skin contact (Haddadian et al., 2013; Verma et al., 2021). Diarrhoea and

vomiting may also result from it. Death may ensue from prolonged exposure to MO (Eljiedi and Kamari, 2017). Dyes when discharged into natural water system, brings toxicological problems along with them, making them unfit for human consumption (Liu et al., 2012). Therefore, treatment of dyes form the wastewater very important before being discharged into natural water bodies. Treatment of dyes may involve any of the physical, biological or chemical processes some of which include; flocculation, ion-exchange, ozonation, precipitation, membrane filtration, biodegradation, etc. But being ineffective and expensive these technologies are less accepted for wide range of treatment of dye in wastewater (Robinson et al., 2001). Adsorption came out superior to other techniques because of its simple design, ease of operation, low initial cost and flexibility. Further this technique can be used to eliminate different types of coloring materials (Adwani et al. 2023; Gupta et al., 2009; Crini et al., 2006). The elevated cost of activated carbon led to the search for low cost, renewable adsorption materials (Bello et al., 2007). Biochar is inexpensive and sustainable adsorbent that can be used to remove organic pollutants from the aqueous solution/watewater. This biochar has a wide range of source including the sludge, agriculture waste, industrial waste etc. Biochar itself has a lot of advantages i.e. large surface area, large pores and rich in functional groups (Zhu et al., 2018). In adsorption process, biochar may hold rich functional groups and have high porosity (Leng et al., 2015).

In the present study, *Lagerstroemia speciosa* (LS) leaves were utilized as raw materials to produce biochar aimed at eliminating CD and AD from the aqueous solutions. The characterization of the biochar was done using SEM, FTIR, PSA and XRD analyzer. The removal of MO and MB from aqueous solution was carried out by the batch adsorption process. Various adsorption isotherms such as Langmuir isotherm (LI), Freundlich isotherm (FI), Temkin isotherm (TI), Dubinin- Radushkevich isotherm (D-RI) and kinetics pseudo-first-order (PFO), pseudo-second-order (PSO), intraparticle diffusion model (IDM) have been applied in this study. Graphs of thermodynamics have also been plotted.

2. Materials and methods

2.1 Materials

The raw materials for preparation of adsorbent i.e. dry leaves of *Lagerstroemia speciosa* was collected from Babasaheb Bhimrao Ambedkar University (BBAU) Lucknow, Uttar Pradesh, India. Thermo-Fisher Scientific, India Pvt. Ltd. provided the chemicals like HCl, NaOH, MB and MO were used in the study.

2.2 Adsorbent preparation

The dry leaves of *Lagerstroemia speciosa* were collected and washed with deionized water to remove the dirt stick to the surface. It was then oven dried for 48 h. The dried material was crushed and grounded to convert into fine powder. This material was then passed through 0.22 mm sieve. Powered material was filled in the crucible and was capped with fitted lid. Crucible was kept into the muffle furnace for pyrolysis at 600^{o}C and was kept constant for 120 min. The sample was allowed to cool inside the muffle furnace till the room temperature. The obtained *Lagerstroemia speciosa* biochar (LSB) was washed with deionized water until all the impurities like bio-oil was removed and was left to oven dry for 12 h. The dried LSB was kept in air tight container and used for additional studies.

2.3 Batch adsorption experiment

Batch adsorption process proceeded with the preparation of stock solutions of MB and MO. Study was done to analyze the outcome of the selected parameters, i.e., adsorbent dose, pH, temperature, concentration and contact time on the adsorption of material from the aqueous solution. The batch study was performed in 100 mL of conical flask using rotary flask shaker. Remaining concentrations of the MB and MO in each flask were analyzed using the UV-spectrophotometer (Systronic India, Model 117) at wavelength 663 nm and 464 nm, respectively. Measurement error was avoided by taking the duplicate reading and using average value for the equilibrium concentration. The adsorption percentage and adsorption capacity of dyes were governed by the following Eqs. (1) and (2), respectively.

$$\textbf{Adsorption (\%)} = \frac{(C_0 - C_e)}{C_0} \times 100 \quad \textbf{(1)}$$

$$\textbf{Adsorption Capacity } (q_t) = \frac{(C_0 - C_e)}{M} \times V \quad \textbf{(2)}$$

where, C_0 is original concentration (mg/L), Ce is final concentration at time t (mg/L), V is solution volume in L, M (g) is mass of adsorbent.

2.4 Characterization of the material

The morphology of surface and elemental composition of the biochar was observed using SEM with EDX (JEOL JSM-6490 LV, Japan). FTIR (Thermo-Scientific Nicolet-6700, USA) was used to detect surface functional groups. For the analysis of the particle size distribution Zeta nanosizer (Malvern Zetasizer nanoseries ZS90) was used. XRD (D8 Advance Eco, Bruker Germany) was also done for the characterization of the biochar. To determine surface neutrality of the LSB, pHzpc was performed using 0.01M NaCl aqueous solution at different pH values (2-10**)** fixed with 0.1M NaOH and 0.1M HCl.

Table 1 Elemental composition of the LSB

Element	Weight%	Atomic%
C K	50.92	61.80
O K	36.76	33.50
Na K	0.58	0.37
Mg K	2.90	1.74
Si K	2.45	1.27
K K	1.72	0.64
Ca K	1.16	0.42
Pt M	3.51	0.26
Total	100	100

3. Results and discussion

3.1 Batch study

3.1.1 Effect of dose

In order to perform batch adsorption study, a cationic dye (CD) and an anionic dye (AD) were taken in 100 mL conical having dose containing 0.5g/L to 3.5 g/L in order to determine the ideal amount of the adsorbent needed for efficient dye removal at room temperature (except temperature study) and at pH 7 (except pH study). Consequently, maximum removal for MB was observed at 1 g/L that is 96 % and for MO at 3 g/L that is 93.7 %. After that, the usage of dose above this showed no significant rise in the capacity of adsorption due to aggregation of particles which hinder further adsorption. The lower of MO was due to presence of charge present on the surface of biochar. As the dose increased further the removal % was started declining shown in Fig.1 (A). At room temperature the solution was put at rotatory flask shaker at 250 rpm for 6 H to reach the equilibrium. Additionally, at first the adsorption rate was extremely high because there are so many unoccupied sites available on the surface of adsorbent. The adsorption capacities of both dyes at time t were calculated using given formula (Eq. 3):

$$Q_e\left(\frac{mg}{g}\right) = (C_0 - C_e) * V/m \qquad (3)$$

Where Qe= adsorption capacity, C_0 and C_t are initial and final concentration respectively, m is dose used in g/L and V is volume of solution in L.

3.1.2 Effect of different concentration and contact time

To see the effects of concentration on adsorption, MO and MB solutions of different concentrations were prepared in the range of 10 to 50 mg/L. The amount of adsorbents used for the removal of MO and MB were 3g/L and 1g/L, respectively. Batch study was carried out in a 100 mL conical. The study was performed for two hours. After 90 min the adsorption stabilizes and reached to equilibrium state.

The maximum removal of both dyes (96% for MB and 94% for MO) was attained at 90 minutes of contact time The high removal of MB was noted in contrast to MO as a result of an increasing contact time between the opposite charges on both MB and LSB (Verma et al., 2021). It was found that when concentrations of MB and MO were increased from 10 mg/L to 50 mg/L, then the removal efficiencies dropped from 96% to 33% and 94% to 26%, respectively as shown in Fig.1 B and C. The possible explanation for this could be higher initial dye concentration occupied the adsorption sites on adsorbent surface and become saturated.

3.1.3 Effect of pH

The influence of pH on adsorption was investigated using range of solution pH values varying from 2 to 10. The pH of solution was maintained using 0.1 M HCI and 0.1 M NaOH solutions and maximum adsorption at different pH was analyzed. The outcome showed no discernible shift in the removal percentage of both dyes over time, confirming the stability of process of adsorption (De et al., 2020). However, MO's adsorption capacity is lower than MB's because the same charge present on the surface of adsorbent and adsorbate which generates repulsion. The capacity of adsorption was 2.4 mg/g for MO as shown in Fig.1C and 9.8 mg/g for MB as predicted in Fig. 1 (D).

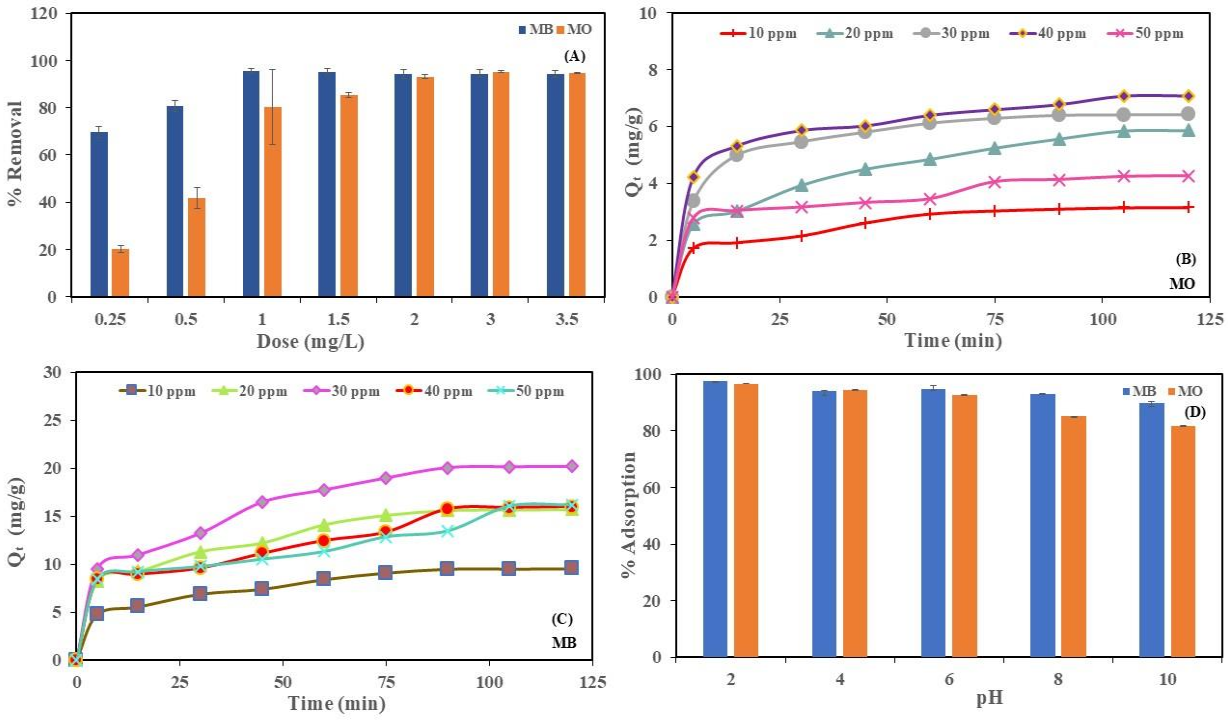

Fig. 1 Effect of (A) dose taken for MB and MO, (B) and (C) shows different concentration at different time interval for MB and MO, respectively, and (D) shows effect of different pH values on MB and MO dyes

3.1.4 Effect of temperature

Another significant parameter is temperature which affects the adsorption capacity. To observe the effect of temperature on adsorption, studies have been done at four different temperatures that are 25°C, 35ºC, 45ºC and 55°C. It was

observed that on increasing temperature, the adsorption capacity was also increased. The reason for this is, the adsorbent surface has specific adsorptive sites that need a specific temperature to become effective/activate. A high temperature is needed to activate the adsorptive sites of the adsorbents (Nordin et al., 2021). In this case, abundance of active sites were present at high temperature which provide more sites available for the adsorbate to bind on the surface of LSB. At 25°C adsorption is lowest and at 55°C adsorption percentage was observed. It implies that the reaction process is endothermic. At temperature increased from 25°C to 55°C the removal percentage was reached to 99.08% for MB. The % removal of MO was found to be lower than that of MB. The adsorption capacity of MB is 9.9 mg/g and that of MO is 3.18 mg/g as shown in Fig.2 (A) and (B). It happened due to the fact that there is similar charge present on the surface of adsorbent and adsorbate which causes repulsion between MO and LSB

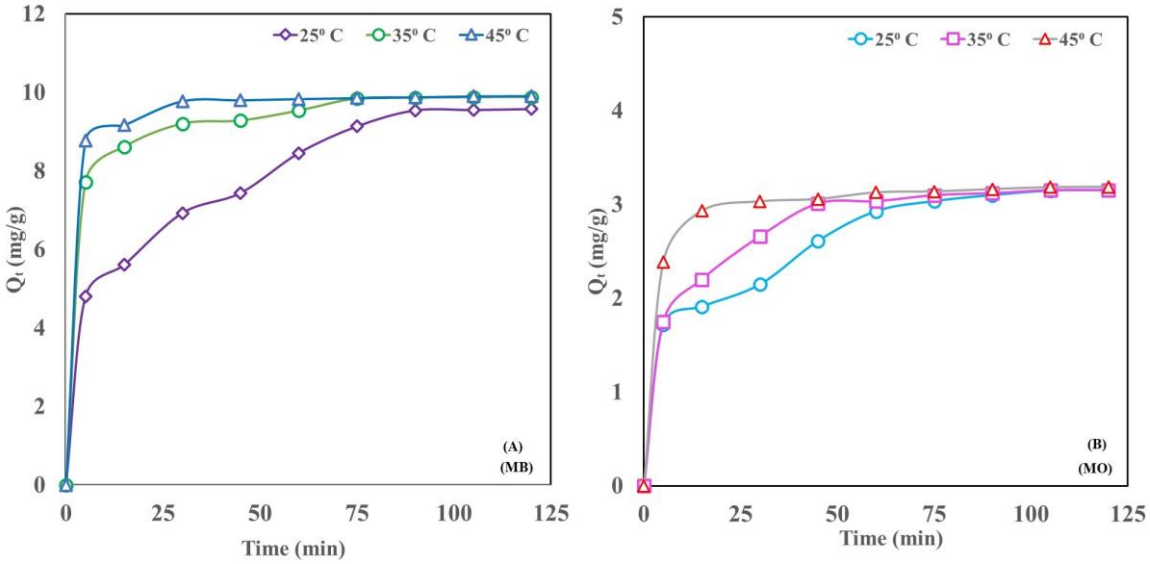

Fig. 2 Effect of different temperature on the adsorption of MB (A) and MO (B) on the surface of LSB

3.2 Characterization of adsorbent

3.2.1 SEM and EDS analysis

The SEM analysis was conducted to assess the size, shape and surface morphology of synthesized biochar material. The results depicted in Fig.3 reveal that the biochar material exhibit irregular shapes with rough surfaces and possess a significant surface area along with high porosity. EDS analysis performed for elemental analysis of LSB as shown in Table 1 which shows have high carbon content that is 68.34% by weight.

3.2.2 FTIR

The functional group present on material before and after adsorption of MO and MB represented by FTIR spectrum which is displayed in Fig.3 (B). Before and after adsorption peaks present on LSB was nearly identical and shifts only slightly which shows successful adsorption. The bands 3419 and 3403 corresponds to hydroxyl group of alcohol. 1563 to 1571 corresponds to primary and secondary amine that is N-H stretch. -CH3 bending vibration attributed to the peak 1411 and 1450, 2879, 1218, 879 represented the C-H bonding of aldehyde group, C-N and C-H stretching, respectively.

3.2.3 XRD

XRD is used to determine crystalline or amorphous structure of the prepared biochar materials. The XRD spectrum revels that the biochar is crystalline in nature. The intense peak found at 29.40 corresponds the crystalline nature of material and assigned to silicon dioxide (Mittal et al., 2022). The finer and sharper peaks were discovered at 2θ values of about 21-30º as shown in Fig. 4(A). In addition to confirming the existence of graphene-like structure in the produced biochar material, these peaks for the biochar materials showed the formation of carbonized material. The deflection peaks present at 35.93°, 39.23°, 43.10° represents calcium silicate and diffraction peaks at 47.50° and 48.60° assign to the presence of calcite (Verma and Singh, 2019).

3.2.3 PSA

PSA was accomplished by homogenizing of the biochar by dissolving it in distilled water at room temperature. Plotting obtained result is displayed in Fig. 4(B), which indicates that broad peak were seen between 150-250 nm. This size distribution suggests that the prepared LSB possess a larger surface area, which may have potentially for efficient adsorption of dyes.

3.2.4 Zero-point charge (pH_{zpc})

The pH_{pzc} establishes the point at which the net charge on surface of carbon was zero(De Farias et al., 2020) which are cumulative action of functional group present on biochar. The surface of carbon has a net positive charge when pH is less than pH_{pzc} and vice versa. The pH_{pzc} is determined by using 0.01N NaCl which is then placed in 50 mL conical flask in five distinct flask and maintain the pH of solution between 2 to 10 by using 0.1 M H_2SO_4 and NaOH and solution was shaken for 48 h. After 48 h, the pH of solution was checked. The pH_{pzc} in

the current investigation was found to be 8.8 (Fig. 5) means biochar is basic in nature because of liberation of alkaline minerals like calcium and magnesium during the thermal decomposition of waste biomass by the pyrolysis process (Verma et al., 2019).

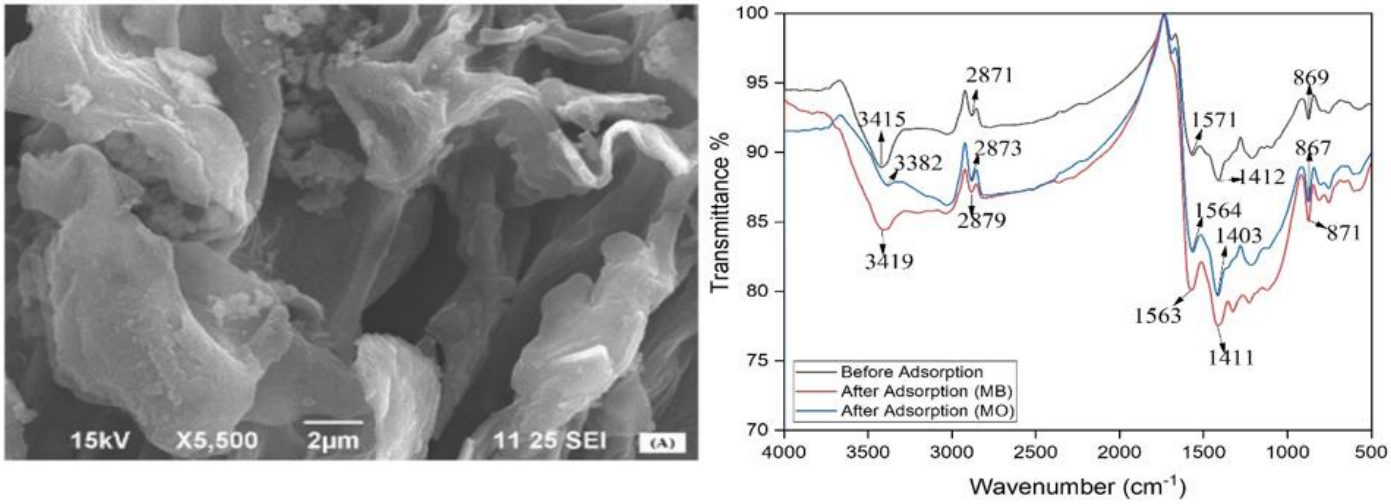

Fig. 3 (A) shows the morphological structure of the surface of biochar, (B) shows the FTIR transmittance spectra of LSB, MB and MO

3.3 Adsorption isotherm

Isotherms are used to explain the adsorption process by comparing the amount of material adsorbed left in the solution. The experimental parameters for the dye adsorption were optimized using the isotherms (Verma et al., 2019). In this study, different isotherm that is Langmuir Isotherm (LI), Freundlich (FI), and Dubinin- Radushkevich (D-R), Temkin (TI) whose values were calculated by using equations 4,5,6 and 7, respectively. R^2 values were used to assess how well the experimental results fit the suggested models shown in Fig.6 and Table 2. LI assuming monolayer and homogeneous adsorption onto an adsorbent surface (Quansah et al., 2020). Heterogeneous sites with a non-uniform distribution are described by the FI model. The value of 1/n fall between 0 and is indication of successful adsorption process (Verma et al., 2021). The LI model was more closely fit by the results from the adsorption for MB (R^2 = 0.9856) and MO (R^2 = 0.952) dye. This assumes that adsorption occurs on a homogeneous surface with a definite number of identical sites where all adsorption sites have the same energy. It simulates that each adsorbate molecule attaches to a single site without interacting with other adsorbed molecules. Since the number of adsorption sites is fixed, once a site is occupied, no further adsorption can occur at that location (Borba et al., 2019).

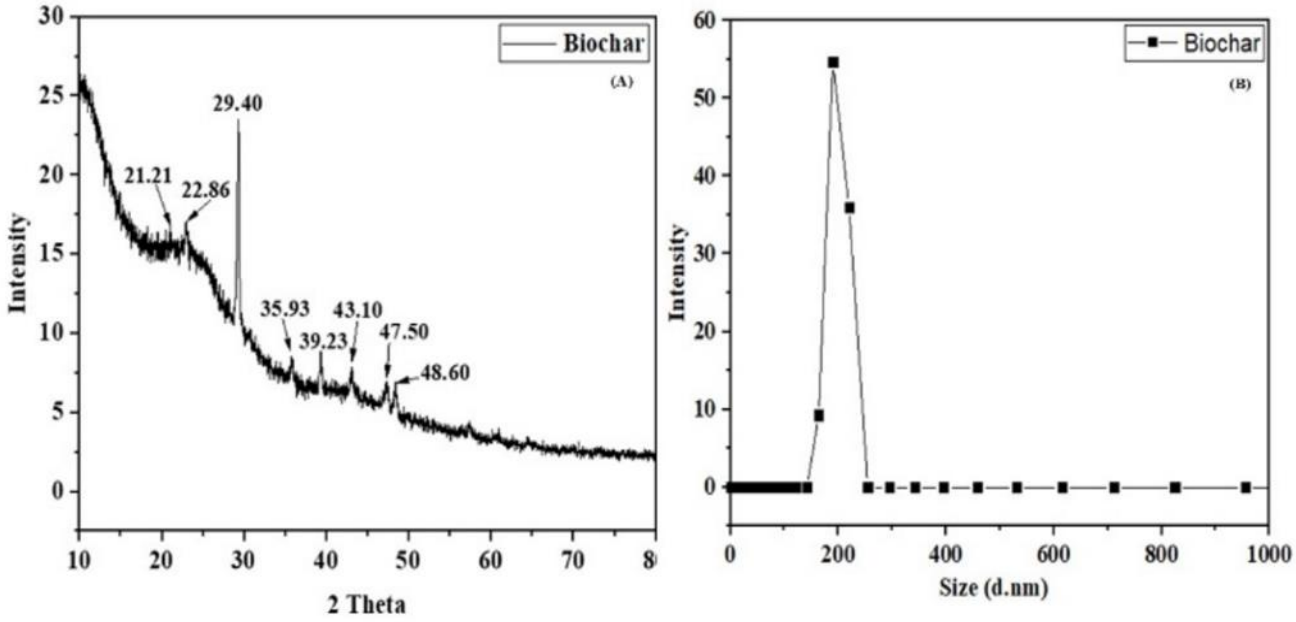

Fig. 4 Spectra showing XRD (A) and PSA (B) showing the size of particle of LSB

According to the corelation coefficient R^2, the models that were used followed the following sequence; Langmuir > Dubinin-Radushkevich > Freundlich > Temkin

$$\frac{Ce}{Qe} = \frac{1}{Qob} + \frac{Ce}{Qo} \quad (4)$$

$$Ln Q_e = \text{Ln}K_F + \frac{1}{n}\ln C_e \quad (5)$$

$$€ = RT \ln\left(1 + \frac{1}{C_e}\right) \quad (6)$$

$$Q_e = \frac{RT}{b}(\ln K_T + \ln C_e) \quad (7)$$

$$E = \frac{1}{\sqrt{2B}} \quad (8)$$

where Qe denotes the adsorbate amount adsorbed (mg/g). Ce is the concentration at equilibrium (mg/L). Qo is denoted as the Langmuir constant and (b) is denoted as the adsorption rate. K_F is adsorption capacity, R and K_T are gas constant and Temkin isotherm constant respectively. E is mean adsorption energy and B is D-RI constant. A graph plotted against Ce and Ce/Qe.

3.4 Adsorption kinetics

Adsorption kinetics is a crucial parameter for understanding the rate at which adsorbate attaches to the adsorbent during the process of adsorption. In this study, PFO (Eq. 9), PSO (Eq. 10) kinetics and IDM were applied to examine the adsorption

$$Log(q_e - q_t) = \log q_e - (K_1/2.303)\, t \quad (9)$$

$$t/q_t = 1/K_2 q_e^2 + \frac{1}{qe} * t \quad (10)$$

mechanism of both dyes on the surface of LSB. PFO determined by interaction between the adsorbent and adsorbate whereas according to pseudo-second-order the rate at which solute adsorption changes is closely correlated with the change in the concentration of adsorptive and saturated solids over time (Verma et al., 2021). Both PFO and PSO provided a good fit to experimental data of MB shown in Table 3 whereas PSO fitted for MO removal as predicted by the value of R^2 shown in Fig. 7. On the basis of available literature (Mittal et al., 2022), adsorption is chemical in nature that is there is strong electrostatic attraction between adsorbent and adsorbate.

Where q_e and q_t denotes amount of MO and MB adsorbed on LSB at equilibrium and time t respectively, K_1 and K_2 are constant for PFO and PSO respectively. The graph was plotted against time and log (Q_e-Q_t) for PFO and t and t/Q_t for PSO.

Table 2 Represent Isotherm parameter for removal of MB and MO using LSB

Isotherm models	Parameters	Adsorbates	
		MB	MO
Langmuir	**Q_0 (mg/g)**	13.66	4.33
	B (L/mg)	-0.0067	-0.111
	R^2	0.98	0.95
Freundlich	**n**	10.01	9.5
	K_F (mg/g)	11.9	4.2
	R^2	0.4	0.3
Temkin	**b (J/mol)**	1.2	0.5
	c	12.4	4.5
	K_t (L/g)	2578	14283
	R^2	0.31	0.239
D-R	**Q_m (mg/g)**	1.023	0.5729
	E (KJ/mol)	0.00035	0.00045
	R^2	0.72	0.65

Table 3 Kinetics parameters represent removal of MB and MO using LSB

Adsorbates		PFO			PSO		
	C_0 (mg/L)	**Q_e (mg/g)**	**K_1 (min^{-1})**	**R^2**	**Q_e (mg/g)**	**K_2 (g/mg/ min)**	**R^2**
MB	10	9.54	0.028	1	10.59	0.0073	0.99
	20	21.01	0.042	0.95	17.33	0.00466	0.99
	30	21.6	0.017	0.98	22.72	0.002976	0.99
	40	20.4	0.039	0.95	17.98	0.0029	0.96
	50	13.4	0.017	1	17.42	0.002969	0.93
MO	10	2.6	0.0079	0.96	3.46	0.024	0.99
	20	4.7	0.0054	0.97	6.57	0.009	0.98
	30	19.3	0.020	0.67	6.75	0.024	0.99

	40	3.86	0.0054	0.91	7.38	0.019	0.99
	50	16.5	0.019	0.50	4.53	0.021	0.98

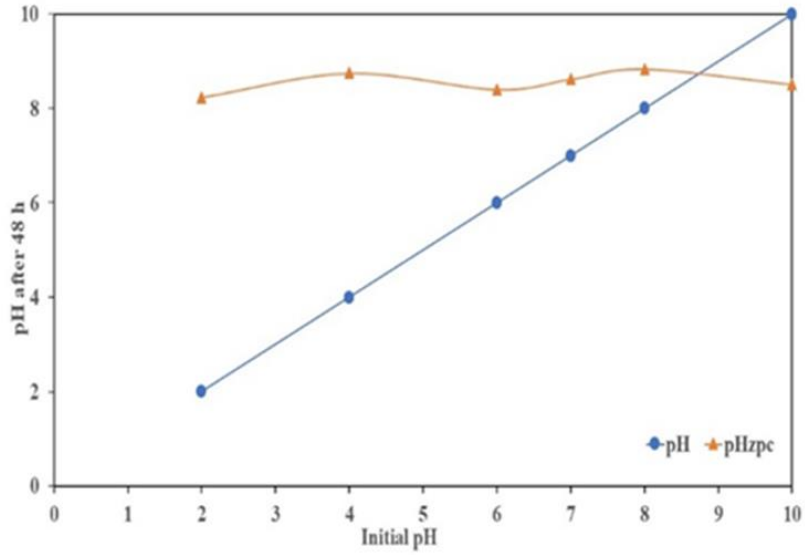

Fig. 5 Graph shown initial and final pH after 48 h

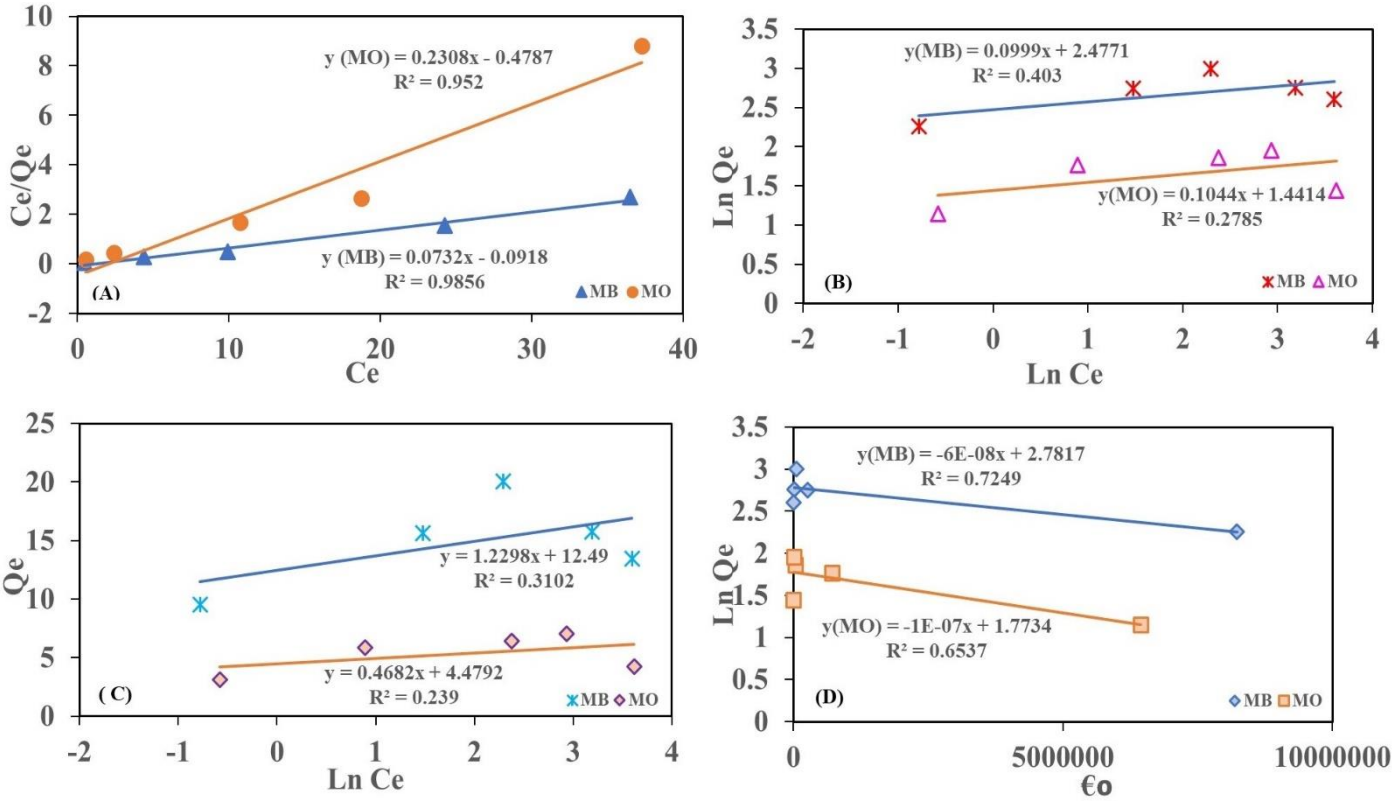

Fig. 6 Different Isotherm model for MB and MO showing Langmuir (a) plot against C_e and C_e/Q_e, Freundlich (b) plotted against LnC_e/LnQ_e, Temkin (c) plotted between LnC_e and Q_e, Dubinin-Radushkevich (d) between ϵ_0 and Ln

3.5 Thermodynamics

The adsorption process was accomplished at different temperature that is 25ºC, 35º 45ºC and 55ºC to better understand the impact of heat on adsorption of MB and MO on LSB. The different parameters enthalpy (ΔH^o), entropy (ΔS^o)

and Gibbs free energy (ΔG^o) were calculated with the help of following Eq. 11:

$$\Delta G^o = \Delta H^o - T\Delta S^o \quad (11)$$

The positive value of ΔH^o (enthalpy change) predicted endothermic process and positive value of ΔS^o (entropy change) revealed the randomness and high stability without any structural change (Navarathna et al., 2019; Mishra et al., 2019). Spontaneous adsorption of dyes were confirmed by the negative value of ΔG^o (gibb's free energy) and the decreasing trend of value with an increasing the temperature, it is good indication that the adsorption process is favourable (Quansah et al., 2020). The value of ΔH^o more than 40 KJ/mol incase of MB, it is characterized by strong bond and is the indication that the process the chemisorption whereas incase of MO value of ΔH^o is less than 40 KJ/mol which indicated the process is physisorption and there is weak bonding (Table 4) between adsorbent and adsorbate (Tonucci et al., 2015; Ghosh et al., 2021). By the help of Fig. 8 the value of thermodynamics values were calculated which again confirmed interaction between adsorbent and adsorbate molecules. In Fig. 8 (C) graph was plotted against LnKC and 1/T which does not pass through the origin at each concentration which exhibited that intra-particle diffusion not only the rate-limiting factor (Gautam et al., 2018). The values were calculated using Eq.12.

$$Q_t = K_i t^{1/2} + C \quad (12)$$

where C is related to boundary layer effect and Ki is intraparticle diffusion constant and graph is plotted against lnKc and 1/T.

4. Mechanism showing interaction

Fig. 9 shows the mechanism related to the adsorption of MB and MO on surface of LSB. The adsorption occurs due to different interaction between the surface of biochar and MB and MO. Hydrogen bond, complexation of surface, electrostatic interaction are major interaction mechanism was involved for the adsorption of dyes onto LSB. Hydrogen bonds were formed between hydroxyl group present on the LSB and dyes molecules (Modwi et al., 2022). Due to negatively charged hydroxyl group and positive charge present on the surface of dye cause strong electrostatic attraction which exhibited high removal of pollutants. The rough surface of material enhanced the rate of adsorption as confirmed by SEM (Sirajudheen et al., 2020; Ghosh et al., 2021). Adsorption process of dye onto biochar surface is strongly bounded by electrostatic interaction which is again confirmed because the adsorption process is well fitted in pseudo-second order as shown in Table 3 (Vigneshwaran et al., 2021).

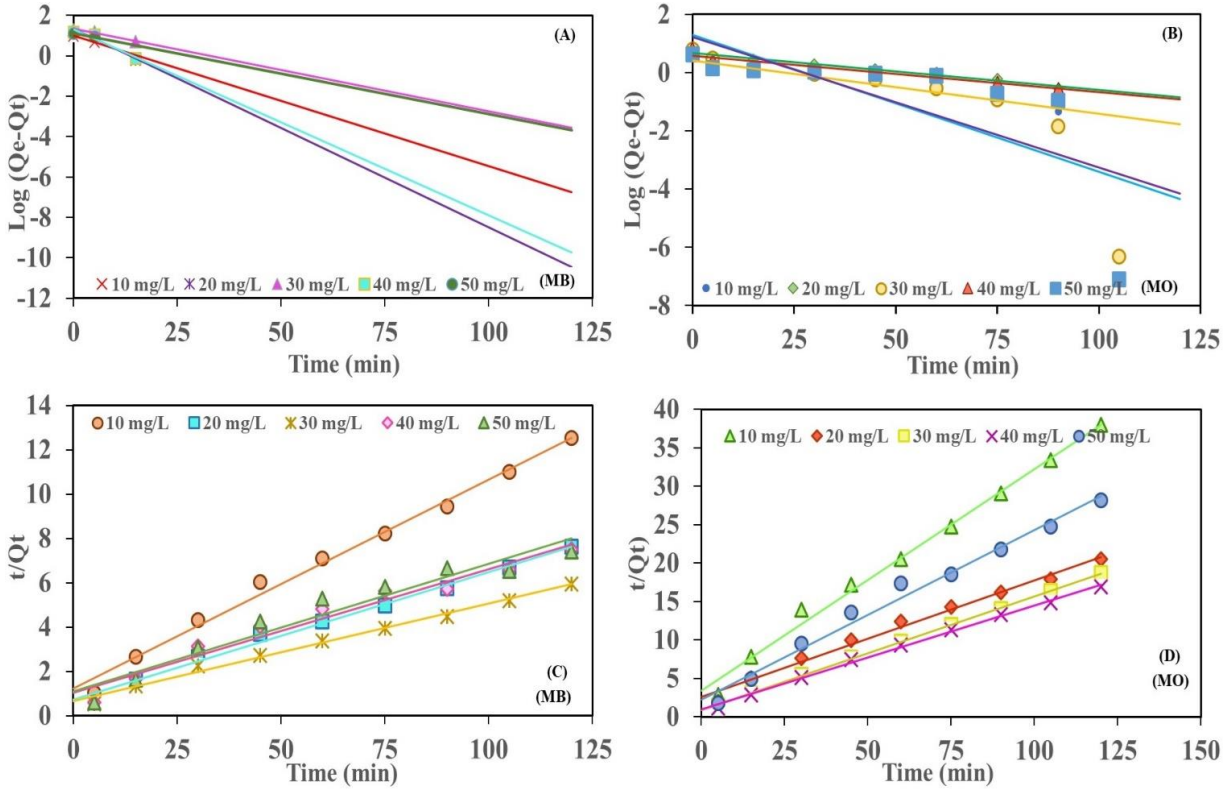

Fig. 7. (A) and (B) showing pseudo-first order for MB and MO respectively plotted between time and log (Q_e-Q_t), (C) and (D) showing PSO for MB and MO removal, respectively formed against time t and t/Q_t

Table 4 Thermodynamics parameter show enthalpy change, entropy and Gibb's free energy

Adsorbates	Parameters of thermodynamics			
	Temperature (K)	ΔGº(KJ/mole)	ΔHº(KJ)	ΔSº(KJ)
MB	298	-61.99	54.09	0.208
	308	-64.08		
	318	-66.16		
MO	298	-13.3	9.12	0.447
	308	-13.7		
	318	-14.2		

5. Conclusion

From the study it can be presume that LSB is a highly effective adsorbent for removing MB about 95% and MO about 93% from its aqueous solution. There was no major effect of pH was observed on the percentage removal of MB and MO by LSB. It was observed that the removal was impacted by high concentration of dyes, when the concentration of dyes was increased then the removal percentage was decreased. Langmuir isotherm was best fitted than Freundlich, Temkin and D-R isotherm. In case of MB, adsorption process was followed both the kinetics model whereas in case of MO pseudo-second-order fitted well. The value of enthalpy was found to be higher for MB which indicates strong bonding between LSB and MB but In case of MO the value of enthalpy was observed less which is a sign of weak bonding (physisorption) between LSB and MO molecule. Negative value of ΔGº confirmed the spontaneous possibility of adsorption process. The adsorption capacity was found to be higher incase of MB than that of MO which confirmed the LSB is very effective adsorbent to remove cationic dye than that of anionic.

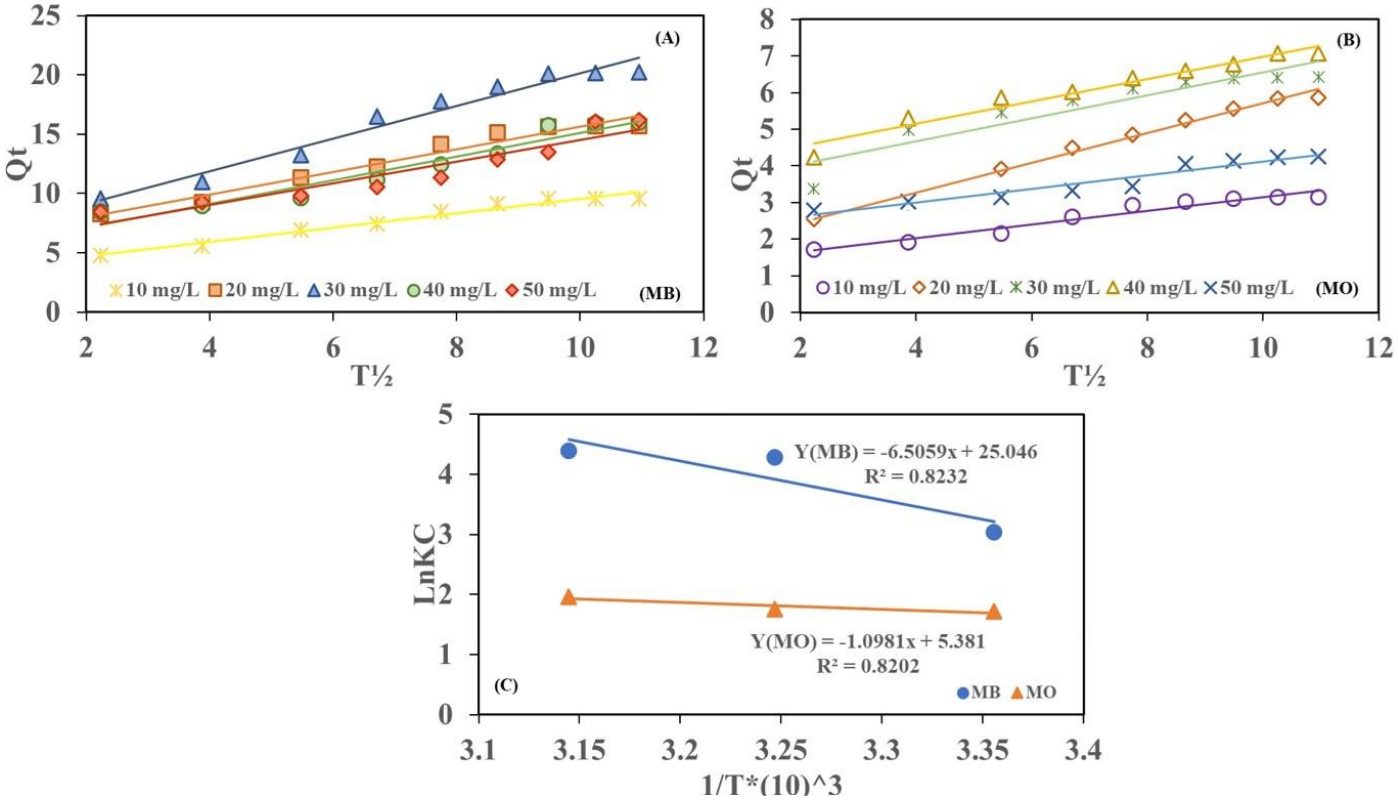

Fig. 8 (A) and (B) predicted intraparticle- diffusion model for MB and MO, respectively, (C) represent effect of enthalpy change, entropy and gibb's free energy on adsorption process for MB and MO.

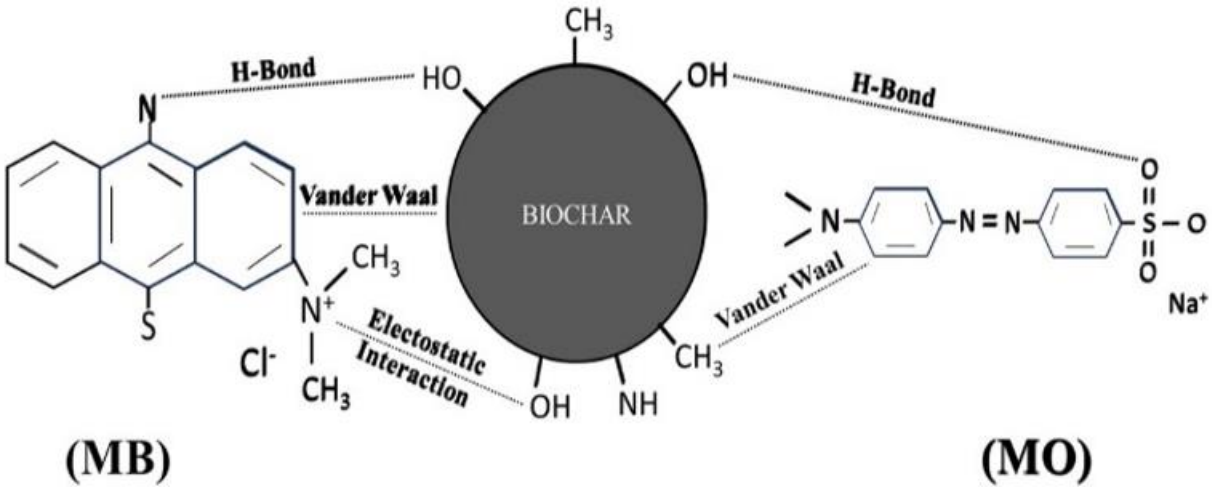

Fig. 9 Mechanism showing the interaction between dye molecule and LSB

Acknowledgement
The authors are thankful to UGC (University Grant commission), New Delhi, India for providing JRF fellowship during the research work.

Funding
The research work did not receive any funding from any public, commercial or not-for-profit sectors.

Author credit statement
Pooja Adwani (Research Scholar) has prepared, conceptualized the draft and done analysis, Bhanushree and Meenakshi performed experiments, Shakti Singh (Edited the script), Jiwan Singh (Supervisor) has reviewed and validated the manuscript.

Conflict of interest
Authors have no conflict of interest.

References

Adwani, P., Singh, J., 2023. Production of biochar from different feedstocks using various methods and its application for the reduction of environmental contaminants: a review. J. Appl. Sci. Innov. Technol. 2 (1), 18-24.

Albadarin, A.B., Collins, M. N., Naushad, M., Shirazian, S., Walker, G., Mangwandi, C., 2017. Activated lignin-chitosan extruded blends for efficient adsorption of methylene blue. Chem. Eng. J., 307, 264-272.

Alhujaily, A., Yu, H., Zhang, X., Ma, F., 2020. Adsorptive removal of anionic dyes from aqueous solutions using spent mushroom waste. App. Water Sci. 10(7), 1-12.

Bello, O.S., Adegoke, K. A., Olaniyan, A. A., Abdulazeez, H., 2015. Dye adsorption using biomass wastes and natural adsorbents: overview and future prospects. Desalination Water Treat. 53(5), 1292-1315.

Bharagava, R.N., 2021. Degradation mechanism and toxicity reduction of methyl orange dye by a newly isolated bacterium Pseudomonas aeruginosa MZ520730. J. Water Process. Eng. 43, 102300.

Borba, L.L., Cuba, R.M.F., Terán, F.J.C., Castro, M.N., Mendes, T.A., 2019. Use of adsorbent biochar from Pequi (Caryocar Brasiliense) husks for the removal of commercial formulation of glyphosate from aqueous media. Braz. Arch. Biol. Technol. 62, e19180450.

Crini, G., 2006. Non-conventional low-cost adsorbents for dye removal: a review. Bioresour. Technol. 97(9), 1061-1085

De Farias S., C.E., da Gama, B.M.V., da Silva Gonçalves, A. H., Medeiros, J. A., de Souza Abud, A. K., 2020. Basic-dye adsorption in albedo residue: Effect of pH, contact time, temperature, dye concentration, biomass dosage, rotation and ionic strength. J. King Saud Univ. Eng. Sci. 32(6), 351-359.

Eljiedi, A.A.A., Kamari, A., 2017. Removal of methyl orange and methylene blue dyes from aqueous solution using lala clam (Orbicularia orbiculata) shell. In AIP Conference Proceedings 1847 (1), AIP Publishing.

Gautam, A., Rawat, S., Verma, L., Singh, J., Sikarwar, S., Yadav, B. C., Kalamdhad, A. S. 2018. Green synthesis of iron nanoparticle from extract of waste tea: An application for phenol red removal from aqueous solution. Environ. Nanotechnol Monit. Manag. 10, 377-387.

Ghosh, I., Kar, S., Chatterjee, T., Bar, N., Das, S. K., 2021. Adsorptive removal of Safranin-O dye from aqueous medium using coconut coir and its acid-treated forms: adsorption study, scale-up design, MPR and GA-ANN modeling. Sustain. Chem. Pharm.19, 100374.

Gupta, V.K., 2009. Application of low-cost adsorbents for dye removal–a review. J. Environ. Manage. 90(8), 2313-2342.

Haddadian, Z., Shavandi, M.A., Abidin, Z.Z., Ahmadun, F.R., Ismail, M.H.S., 2013. Removal methyl orange from aqueous solutions using dragon fruit (Hylocereusundatus) foliage. Chem. Sci. Trans. 2(3), 900-910.

Kishor, R., Purchase, D., Ferreira, L.F.R., Mulla, S.I., Bilal, M., Bharagava, R.N., 2020. Environmental and Health

Hazards of Textile Industry Wastewater Pollutants and Its Treatment Approaches. In: Hussain, C. (eds) Handbook of Environmental Materials Management. Springer, Cham. https://doi.org/10.1007/978-3-319-58538-3_230-1

Leng, L., Yuan, X., Huang, H., Shao, J., Wang, H., Chen, X., Zeng, G., 2015. Bio-char derived from sewage sludge by liquefaction: Characterization and application for dye adsorption. Appl. Surf. Sci. 346, 223-231.

Liu, T., Li, Y., Du, Q., Sun, J., Jiao, Y., Yang, G., Wu, D., 2012. Adsorption of methylene blue from aqueous solution by graphene. Colloids Surf. B., 90, 197-203.

Long, Q., Zhang, Z., Qi, G., Wang, Z., Chen, Y., Liu, Z. Q., 2020. Fabrication of chitosan nanofiltration membranes by the film casting strategy for effective removal of dyes/salts in textile wastewater. ACS Sustain. Chem. Eng. 8(6), 2512-2522.

Mishra, S., Yadav, S.S., Rawat, S., Singh, J., Koduru, J. R., 2019. Corn husk derived magnetized activated carbon for the removal of phenol and para-nitrophenol from aqueous solution: Interaction mechanism, insights on adsorbent characteristics, and isothermal, kinetic and thermodynamic properties. J. Environ. Manag. 246, 362-373.

Mittal, J., Ahmad, R., Ejaz, M. O., Mariyam, A., Mittal, A., 2022. A novel, eco-friendly bio-nanocomposite (Alg-Cst/Kal) for the adsorptive removal of crystal violet dye from its aqueous solutions. Int. J. Phytoremediation 24(8), 796-807.

Modwi, A., Khezami, L., Ghoniem, M.G., Nguyen-Tri, P., Baaloudj, O., Guesmi, A., Assadi, A. A. 2022. Superior removal of dyes by mesoporous MgO/g-C3N4 fabricated through ultrasound method: Adsorption mechanism and process modeling. Environ. Res. 205, 112543.

Navarathna, C.M., Karunanayake, A.G., Gunatilake, S.R., Pittman Jr, C. U., Perez, F., Mohan, D., Mlsna, T., 2019. Removal of Arsenic (III) from water using magnetite precipitated onto Douglas fir biochar. J. Environ. Manag. 250, 109429.

Nordin, A.H., Wong, S., Ngadi, N., Zainol, M.M., Abd Latif, N. A. F., Nabgan, W., 2021. Surface functionalization of cellulose with polyethyleneimine and magnetic nanoparticles for efficient removal of anionic dye in wastewater. J. Environ. Chem. Eng. 9(1), 104639.

Oz, M., Lorke, D.E., Hasan, M., Petroianu, G.A. 2011. Cellular and molecular actions of methylene blue in the nervous system. Med. Res. Rev. 31(1), 93-117.

Quansah, J.O., Hlaing, T., Lyonga, F.N., Kyi, P.P., Hong, S. H., Lee, C. G., Park, S. J., 2020. Nascent rice husk as an adsorbent for removing cationic dyes from textile wastewater. Appl. Sci. 10(10), 3437.

Robinson, T., McMullan, G., Marchant, R., Nigam, P., 2001. Remediation of dyes in textile effluent: a critical review on current treatment technologies with a proposed alternative. Bioresour. Technol. 77(3), 247-255

Russo, V., Masiello, D., Trifuoggi, M., Di Serio, M., Tesser, R. 2016. Design of an adsorption column for methylene blue abatement over silica: From batch to continuous modeling. Chem. Eng. J. 302, 287-295.

Shabaan, O. A., Jahin, H. S., Mohamed, G.G. 2020. Removal of anionic and cationic dyes from wastewater by adsorption using multiwall carbon nanotubes. Arab. J. Chem. 13(3), 4797-4810.

Sirajudheen, P., Nikitha, M.R., Karthikeyan, P., Meenakshi, S. 2020. Perceptive removal of toxic azo dyes from water using magnetic Fe3O4 reinforced graphene oxide–carboxymethyl cellulose recyclable composite: Adsorption investigation of parametric studies and their mechanisms. Surf. Interfaces 21, 100648.

Su, Y., Jiao, Y., Dou, C., Han, R., 2014. Biosorption of methyl orange from aqueous solutions using cationic surfactant-modified wheat straw in batch mode. Desalin. Water Treat. 52(31-33), 6145-6155.

Tonucci, M.C., Gurgel, L.V.A., de Aquino, S. F., 2015. Activated carbons from agricultural byproducts (pine tree and coconut shell), coal, and carbon nanotubes as adsorbents for removal of sulfamethoxazole from spiked aqueous solutions: Kinetic and thermodynamic studies. Ind. Crops Prod., 74, 111-121.

Verma, L., Singh, J., 2019. Synthesis of novel biochar from waste plant litter biomass for the removal of Arsenic (III and V) from aqueous solution: A mechanism characterization, kinetics and thermodynamics. J. Environ. Manage. 248, 109235.

Verma, M., Tyagi, I., Kumar, V., Goel, S., Vaya, D., Kim, H., 2021. Fabrication of GO–MnO2 nanocomposite using hydrothermal process for cationic and anionic dyes adsorption: Kinetics, isotherm, and reusability. J. Environ. Chem. Eng. 9(5), 106045.

Vigneshwaran, S., Sirajudheen, P., Karthikeyan, P., Meenakshi, S. 2021. Fabrication of sulfur-doped biochar derived from tapioca peel waste with superior adsorption performance for the removal of Malachite green and Rhodamine B dyes. Surf. Interfaces 23, 100920.

Zhu, Y., Yi, B., Yuan, Q., Wu, Y., Wang, M., Yan, S., 2018. Removal of methylene blue from aqueous solution by cattle manure-derived low temperature biochar. RSC Adv. 8(36), 19917-19929.

Cite this article:

Adwani, P., Bhanusree, B., Meenakshi, Singh, S., Singh, J., 2024. Comparative study on removal of cationic and anionic dyes using biochar synthesized from dry leaves of *Legerstroemia speciosa*: Kinetics, isotherm and thermodynamic study. J. Appl. Sci. Innov. Technol. 3 (2), 86-96.